International Journal of Ecology and Environmental Sciences 49: 217-230, 2023
ISSN: 2320-5199 (Online); https://doi.org/10.55863/ijees.2023.2626



# Spatial-Temporal Analysis of Physio-Climatic Changes in Tawang-Chu River Basin, Eastern Himalaya in India

**OM JEE RANJAN[1,8]*, USHA RANI[1,9], SUBHASH ANAND[1], B.W PANDEY[1], GEOFFREY MUKWADA[2,3], PATRICIO DE LOS RIOS ESCALANTE[4,7], DILEK EREN AKYUZ[5] AND ASHWAJEET CHAUDHARY[6]**

*[1]Department of Geography, Delhi School of Economics, University of Delhi, Delhi, India*
*[2]Department of Geography, University of the Free State, South Africa*
*[3]Department of Geography & W.A. Franke College of Forestry & Conservation, University of Montana, Missoula, USA*
*[4]Department of Biological and Chemical Sciences, Faculty of Natural Resources, Catholic University of Temuco, Temuco, Chile*
*[5]Department of Civil Engineering, Istanbul University-Cerrahpasa, 34320 Avcilar, Istanbul, Turkey*
*[6]Department of Geography University of Allahabad, Allahabad, Uttar Pradesh, India*
*[7]Department of Biological and Chemical Sciences/Environmental Studies Nucleus, Faculty of Natural Resources, Catholic University of Temuco, Temuco, Chile*
*[8]Department of Geography, Miranda House, University of Delhi, Delhi, India*
*[9]Institution of Eminence, University of Delhi, Delhi, India*
E-mail: omjeeranjan@gmail.com, ushar489@gmail.com, sanandpvs@gmail.com, bwpdsegeo@gmail.com, mukwadaG@ufs.ac.za, prios@uct.cl, deakyuz@gmail.com, ashwajeetchaudhary@gmail.com
***Corresponding Author**

**ABSTRACT**
The Tawang-Chu River Basin of the eastern Himalayas is a heterogenous region that is highly vulnerable to climate change. The changing temperature patterns in this mountain river basin play a vital role in changing the ecological system and inter-ecological nexus. Landsat satellite images were used to analyze spatio-temporal changes in Land Use and Land Cover (LULC) patterns in the basin. The changing trends of Land Surface Temperature (LST) and Normalized Difference Vegetation Index (NDVI) were analyzed (at intervals of five years) using Landsat data. Changes in rainfall trends were analyzed using the Mann-Kendall test. The results show that fluctuations in annual temperature and increasing rainfall uncertainties are affecting LULC vegetation health.

**Key words**: Eastern Himalaya; Tawang-Chu River Basin; Land Surface Temperature; NDVI; Rainfall Trend; Mann-Kendall test

## INTRODUCTION

The mountain ecosystem is unique and distinct from other ecosystems. A combination of various factors like rugged topography, harsh climatic conditions, inaccessibility, remoteness reduces livelihood options and sustainability in Eastern Himalaya high-altitude river basins (Ranjan et al. 2016, Beniston et al. 1997). The Tawang-Chu River Basin is a typical example of this kind of ecosystems. The basin lies between 949 to 6338 metres above sea level (masl) and is characterised by rugged topography, steep slopes and deep incised valleys. In this basin, it is an established fact that climatic parameters, along with physiographic features, are changing and the characteristics of ecosystems in the basin are changing alongside food chains (ICIMOD 2008), thus creating new environmental conditions for local communities (Pandey and Prasad 2018). Physio-climatic conditions play a vital role in changing the mountain ecosystem, and its impact on human adaptation currently remains a major issue (Fischlin and Bugmann 1994, Dussaillant et al. 2019). Mapping the degree of adaptation requires an evaluation of the changing trends of physio-climatic conditions (Diaz and Bradley 1997, Jones 2019). The analysis of the changing trends can provide information that is useful for human adaptation. For this purpose, the study area was analyzed using Remote Sensing (RS) and Geographic Information

System (GIS) in order to understand the present physio-climatic features of the area in order to compare them with those that prevailed in the past (Diaz et al. 2003, Rahman and Dedieu 1994). Changing physio-climatic trends and pattern are coupled with the simultaneous evolution of the human conditions, hence they are significant in explaining the degree of human adaptation (Villaba 2003). To maintain human adaptation at a desirable level, time scale data analysis could be an appropriate method of analysis (Kohler et al. 2010, Dussaillant et al. 2019, Jones 2019). Human adaptation cannot be measured adequately without assessing changes in physio-climatic conditions. The degree of climate variability determines physiographical features in mountain ecosystems (Whiteman 2000, Dussaillant et al. 2019). Altered physio-climatic conditions have an effect on the state of ecological services and dependent consumers have to adapt to the changing ecology to survive (Fuhrer et al., 2006; Jones, 2019). By assessing climatic indicators, the continuously changing value of ecological services can be understood (Kohler 1949, Marengo 2005). This could be a better approach for human adaptability to physio-climatic changes taking place in the valley (Ranjan et al. 2017). However, as a general rule, it has been observed that the option of changing livelihoods only provides temporary stability (Mishra and Pandey 2019). Therefore, given the above facts, it is the basic objective of this research paper to assess the spatial and temporal changes of physio - climatic conditions in the Tawang-Chu River Basin and their implications for Land Use and Landcover changes, as well as natural resources and related ecosystem services in the basin.

## STUDY AREA

The study area, which covers most of the Tawang-Chu River Basin, covers about 2172 km$^2$ of the Tawang District, one of the 25 districts of the State of Arunachal Pradesh. The Tawang District got its name from the river basin. This region, covered with dense mountain vegetation, predominantly experiences cold and humid climatic conditions. The basin experiences three main seasons: mild summer season (during March to June), a profuse rainy season (from July to October) and an arduous winter season (from November to February: District Statistical Handbook 2015). According to the data from the weather station of Tawang Town, in 2018 and 2019 the recorded minimum temperature was about -5.0$^o$C during winter season (in January) and the maximum temperature was 24$^o$C during summer season (in July), while the average temperature was about 2.0$^o$C in winter and 17.0$^o$C in summer (District Statistical Handbook 2019, Ranjan et al. 2020). As noted above, the study area is a high-altitude mountainous river basin with rugged topography, steep slopes and deep incised valleys. About 56.45% of the Tawang-Chu River Basin is covered in forest, which is limited to the altitude of about 3500 meters of the total forest cover, 366 km$^2$ is very tropical wet and dense rainforest cover, 486 km$^2$ is moderate dense (Tropical Semi Green and Moist Deciduous Forest) and 374 km$^2$ is open alpine forest cover (IUCN 2004). The valley has rich biodiversity and ecological services. Ecological service-chains start with flora and fauna generated by its complex bonds to build a systematic mechanism (Corbet and Hill, 1992), hence, vegetation cover determines the value of ecological services and its nature. Due to the cold and humid climatic conditions which characterize the Tawang-Chu River Basin, cloud cover is prevalent for most of the year, which restricted the use of satellite data to those months when cloud cover was low.

## METHODS

### Toposheets and satellite data

To fulfil the objective of the study, India toposheets 78M/9,10,13,14,15; 83A/1,2,3 was identified and RS data for the areas covered by the toposheets was analysed using ArcGIS. Landsat images, Land Surface Temperature (LST) values and trends for the Normalized Difference Vegetation Index (NDVI) were analysed at five years intervals. RS and ArcGIS were used to perform spatial of land use and land cover changes (LULC) and while trend analyses for LST, daily rainfall and NDVI were performed using Excel. The usage of NDVI is an effective green vegetation quantification method for analysing vegetation health using RS techniques (Carlson and Ripley, 1997). NDVI values were calculated for the years 1990, 1994, 1999, 2004, 2010 and 2017, the same years for which LST values were calculated (as noted below) in order to make a comparative analysis between the variability of LST and NDVI

values.

**Calculation of NDVIs**

NDVI values were calculated using the following equations in which specific bands of satellite images were applicable (Carlson and Ripley 1997).

In Landsat 4-5,

*NDVI = [Band 4 - Band 3]/[Band 4 + Band 3]* .....1

In Landsat 8,

*NDVI = [Band 5 - Band 4]/ [Band 5 + Band 4]* .....2

Basically, this index is based on the chlorophyll detection method. Equation 3 illustrates how NDVI values are calculated.

*NDVI = [NIR - RED]/[NIR + RED]* .....3

where, NIR = Refection in NEAR INFRARED Spectrum, RED = Refection in RED Spectrum.

To the value ranges to determine NDVI and its temporal changes derived from the formula lies between -1.0 to +1.0 in which, the extreme negative value, which will near to -1.0 reflects the presence of water, those near zero or almost to zero (-0.1 to 0.1), are indicative of the presence of snow or barren land or rock. While, higher positive values indicate the presence of vegetation (Valor and Caselles 1996, Ranjan et al. 2020). For an example, 0.89 is close to 1, indicating the presence of dense temperate forest, an indicator of high rainfall. On the other hand, low positive values between 0.1 and 0.3, signify the presence of grassland or shrubs.

The analyses of these variables ensured that the mode, tendency and varying relationships could be understood (Berk et al.1989). The trend for daily rainfall data was analysed for a period of thirty-four years (1985 to 2018) using the Mann-Kendall (MK) test (Mann 1945, Kendall 1975, Gilbert 1987).

**Land Surface Temperature (LST) Data**

Landsat 4 (TM), Landsat 5 (TM) and Landsat 8 OLI/TIRS satellite data can be used as a source of LST data (Laraby and Schott 2018). Landsat 4 and Landsat 5 images have a spatial resolution of 30 meters and consist of seven spectral bands which are used create map for 1990 to 2010 and for maps of 2017, Landsat - 8OLI/TIRS was used. LST data for the years 1990, 1994, 1999, 2004, 2010 and 2017 were used to analyse fluctuations in temperature ranges. Data for these years were largely cloud free. Cloud free Landsat data for years 1995, 2000 and 2005 were not available due to weather disturbances that characterized these years. LST data are related to the radiant surface heat of the land which is measured and calculated by the satellite remote sensor (Becker and Li 1990, Gomis-Cebolla et al. 2018, Romaguera et al. 2018). Radiant heat energy values vary according to the features of the land surface. Every material has a different rate and capacity of heat radiation (Oguz 2013, Gomis-Cebolla et al. 2018, Romaguera et al. 2018). Hence, surface temperature is calculated on the basis of differences in radiative energy emanating from a surface and it depends of the characteristics of the materials found on that surface.

The following section provides a description and the formulas that were used to calculate surface temperature-related data from the Landsat 5 satellite images. Three steps were followed in this process. During the first step, the Digital Numbers (DNs) were converted into radiance values by using the bias and gain values approach (Nerry et al. 1998, Mallick et al. 2017, Liu et al. 2019).

(i) Step 1 involves the conversion of DN into radiance, using the following formula:

$$L\lambda = \left(\frac{(LMAX\lambda - LMIN\lambda)}{(QCALMAX - QCALMIN)}\right) \times \frac{(QCAL - QCALMIN) + LMIN\lambda}{1} \quad ....4$$

where. $L\lambda$ = Spectral Radiance at the sensor's aperture in watts/ ($m^2$ * ster * µm). *QCAL* = it's a digit (in numbers), *LMINë* = Spectral radiance ($L\lambda$) (in minimum value) scale of *QCALMIN*,*LMAX*$\lambda$ = Spectral radiance scales (in maximum value) of *QCALMAX*, *QCALMIN* = Minimum quantized calibrated pixel value (typically = 1), *QCALMAX*= Maximum quantized calibrated pixel value.

(ii) In Step 2 radiance was converted to temperature in Kelvin (which is $^0K$ $^o$*-273.15 = -273.1°C*), without atmospheric corrections, using Equation 2,

$$T = \frac{K2}{In\left(\frac{K_1}{L\lambda}+1\right)} \quad .....5$$

where,

*T* = Effective at-satellite temperature in Kelvin, *K2* = Calibration constant 2, *K1* = Calibration constant 1, *L* = Spectral radiance in watts/ ($m^2$ * ster * µm)

(iii) Step 3 involved the LST calculation. In this step, the temperature was converted from Kelvin into Celsius. which is *0* $^0K$ $^o$*-273.15 = -273.1°C* means

$$C = K - 273.15 \quad .....6$$

For the year 2017, Landsat - 8OLI/TIRS images were

used to calculate LST values. The following procedure was followed in the calculation.

Firstly, the Operational Land Imager (OLI) and Thermal Infrared Sensor (TIRS) (these are installed instruments on the Landsat 8 satellite) were converted into radiance.

$$L\lambda = MLQcal + AL \quad \ldots\ldots\ldots\ldots\ldots\ldots\ldots\ldots\ldots 7$$

where, $L\lambda$= Temperature of atmosphere spectral radiance, *ML* = Band-specific multiplicative rescaling factor from the metadata (RADIENCE MULTI BAND *X* where *X* is the band number), *AL*= Band-specific additive rescaling factor from the metadata (RADIENCE_ADD_BAND_*X*, where *X* is the band number), *Q cal* = Quantized and calibrated standard product pixel values (DN).

Remaining two steps are the same as those noted above (Table 1).

Table 1: Thermal band calibration constants

| Satellite/Sensor | Constant 1 K1watts/ (meter square * ster * μm) | Constant 2 K2 Kelvin |
|---|---|---|
| Landsat - 5 TM | 607.76 | 1260.56 |
| Landsat - 8OLI/TIRS | 774.89 | 1321.08 |

Source: Derved from Landsat 5TM and Landsat 8OLI/TIRS retrival data 2019.

**Rainfall Trend Analysis**

Climatic indicators, including all forms of precipitation are a vital factor affecting physiographical conditions (Longobardi and Villani 2010). The variability of the annual rainfall has a significant role in it (Buishand 1982, Rahman and Begum 2013). Examining the trend of rainfall provides an analytical standard for possible adaptation strategies, especially in high altitude river basin of Eastern Himalaya (Wallis and Moore 1941, Yaning et al. 2009). Thirty-four years daily rainfall data were analysed and tested using Mann Kendall (MK) trend test and Sen's slope estimator (S) (Lehmann 1975, Zar 2010, Nussbaum 2015). This was done in order to check whether rainfall amount has changed over a time and if it has changed to determine the mood of changes (Modarres and Silva 2007, Li 2008, Olivera-Guerra et al. 2020).

***Mann Kendall (MK) trend test***

Rainfall trends were analysed using the Mann-Kendall test. The Null Hypothesis ($H_o$) was that there is no trend change in rainfall, while the alternative Hypothesis ($H_a$) was that there a change in rainfall trend. The Mann-Kendall test is a non-parametric statistical test frequently used for trend analysis of rainfall and temperature time series data (Wald and Wolfowitz 1942, Mohamed and Mukwada 2020). During the Mann-Kendall Test computation procedure, the time series of data points denoted by '***n***' and '***Ti***' and '$T_j$' are other subset of data.

In which,

*i* is 1,2,3,4,5,6,7,....., n-1

and *j* = *i*+1, *i*+2, *i*+3, *i*+4, *i*+5 ....., n

Therefore, the values of the data are evaluated as a time series. According to the MK Test, "if a calculated outcome value from a later time period is higher than a calculated outcome (in digit) from an earlier time period, the statistic S is incremented by 1 on the contrary, if value from a later time period is lower than a value sampled earlier, S is decremented by 1. The net result of all such increases and declines is the final value of S. The initial value of 'S', is assumed to be '0' (it means no significant trend has been found)" (Mann 1945, Kendall1975).

The formula for computation of Man-Kendall Statistical (***S***) Test is:

$$S = \sum_{i=1}^{n-1} \sum_{j=i+1}^{n} sign\,(Tj - Ti) \quad \ldots\ldots\ldots 8$$

Where n = is the number of data point (length of the time series)

$$Sign\,(T_j - T_i) = \begin{cases} 1 \; if \; Tj - Ti > 0 \\ 0 \; if \; Tj - Ti = 0 \\ -1 \; if \; Tj - Ti < 0 \end{cases} \quad \ldots\ldots\ldots 9$$

where, Tj and Ti are the annual values (time series observation in the chronological order) in years j and i and $j > i$, respectively.

The variance has been calculated using Equation 7.

$$Var(S) = \frac{n(n-1)(2n+5) - \sum_{i=1}^{m} t_i(t_i-1)(2ti+5)}{18} \quad \ldots 10$$

where, n = number of data points, m = number of tied groups, and $t_{i=}$ number of ties of extent i.(here tied group is a set of sample which's values are same).

Further, if the sample size (n) is greater than 10 [n > 10] then the following formula is used.

$$Z_s = \begin{cases} \frac{S-1}{\sqrt{Var(S)}}, & if\ S > 0 \\ 0, & if\ S = 0 \\ \frac{S+1}{\sqrt{Var(S)}}, & if\ S < 0 \end{cases} \quad \text{.....11}$$

In line with the above formula, a positive Z value indicates an increasing trend, while a negative Z value denotes a decreasing trend.

In this testing process, á shows significant trend; it means, if, $|Z_s| > Z_{1-á/2}$, the null Hypothesis is rejected and there is some kind of trend in the time series data which's significance level decides the degree of trend in the time series. $Z_{1-á/2}$ is obtained from the standard normal distribution table. To analyze the rainfall trend in 34 years seasonal data significance levels á = 0.01 and á = 0.05 has been used. At the 5% significance level, the null hypothesis of no trend is rejected if $|ZS| > 1.96$ and rejected if $|ZS| > 2.576$ at the 1% significance level.

***Sen's Slope Estimator (S)***

To estimate the magnitude of trend (slope of trend) in time series data, the Sen's Slope Estimator method was used and the following formula was applied.

$$Q_i = \frac{X_j - X_k}{j-k} \quad \text{for i} = 1, \ldots, \ldots, \ldots, \text{N} \text{.....12}$$

where, $X_j$ and $X_k$ are the values at the time point of j and k (in which is j is greater than k e.g. [j > k] respectively.

But there would be two situations in each time period;

1. If only one datum value is present then

N = [n(n-1)]/2 where n = the number of time periods

2. If there are multiple observations in one or more time periods, then

N < [n(n-1)]/2 where n = the number of time periods

The values of *N* for $Q_1$ are graded (ranked) – in in ascending order (smallest to biggest values) and it is computed (Sen's Slope Estimator or slope- median) using Equation 10.

$$Q_{med} = \begin{cases} Q_{[\frac{N+1}{2}]} & \text{if N is odd} \\ \frac{Q_{[\frac{N}{2}]} + Q_{[\frac{N+2}{2}]}}{2} & \text{if N id even} \end{cases} \text{.....13}$$

where, $Q_{med}$ is median values, which shows the trend of reflection which is actually steepness of trend. Further, following formula has been used to see the confidence interval in the slope (Hollander and Wolfe 1973, Gilbert 1987, Mohamed and Mukwada 2020).

$$C_\alpha = Z_{1-\alpha/2}\sqrt{Var(S)} \text{.....14}$$

where, Var (S) is variance $Z_{1-á/2}$ is table of Standard normal Distribution. During computation of this formula, one significance level has been considered – á = 0.05 level. (Partal and Kahya 2006).

## RESULTS AND DISCUSSION

### Trends in LST Tawang-Chu River Basin

The results indicate that LST values for the Tawang-Chu River Basin are changing and impacting the ecology of the basin. A rise in temperature depicts climate change or global warming.

As shown in the results, in 1990 the minimum temperature was -37$^0$C and the maximum temperature ranged between 29 and 30$^o$C. Most of the area had a temperature range of -2 to 10°C. Figure 1 comprises thematic maps that were derived from Landsat images that were analyzed.

The minimum, maximum and mean LST values show a positive temperature trend in the river basin (Fig. 2). In 1999 LST values ranged between -28 and 27°C. In 2004, they ranged from -29 to 26°C (Fig. 2).

In 2010 the minimum temperature was -29°C, while the maximum was 26°C. Following this period of increasing trend of temperature, in 2017, the minimum LST -18°C and maximum LST 32$^o$C were recorded. As shown in the Figure 2, the minimum temperature is gradually increasing from 1990 to 2017. It increased to about 14$^o$C. Similarly, the maximum temperature range also increased by around 4$^o$C during the entire 27-year period. The rise in minimum temperature by about 17-18°C in high the Tawang-Chu River Basin is a serious threat to the basin's ecosystems. This rapid increase in minimum temperature can pose a huge threat to people because it affects livelihoods.

While the rising trend of average maximum-temperature is a comparably low, the trend of rising maximum temperature of land surface is showing statistically significance as $R^2 = 0.521$. It is the coefficient of determination. Changing trend of minimum LST with respect of taken subsequent years (1990-2017) showing steep increasing trend as $R^2 =$

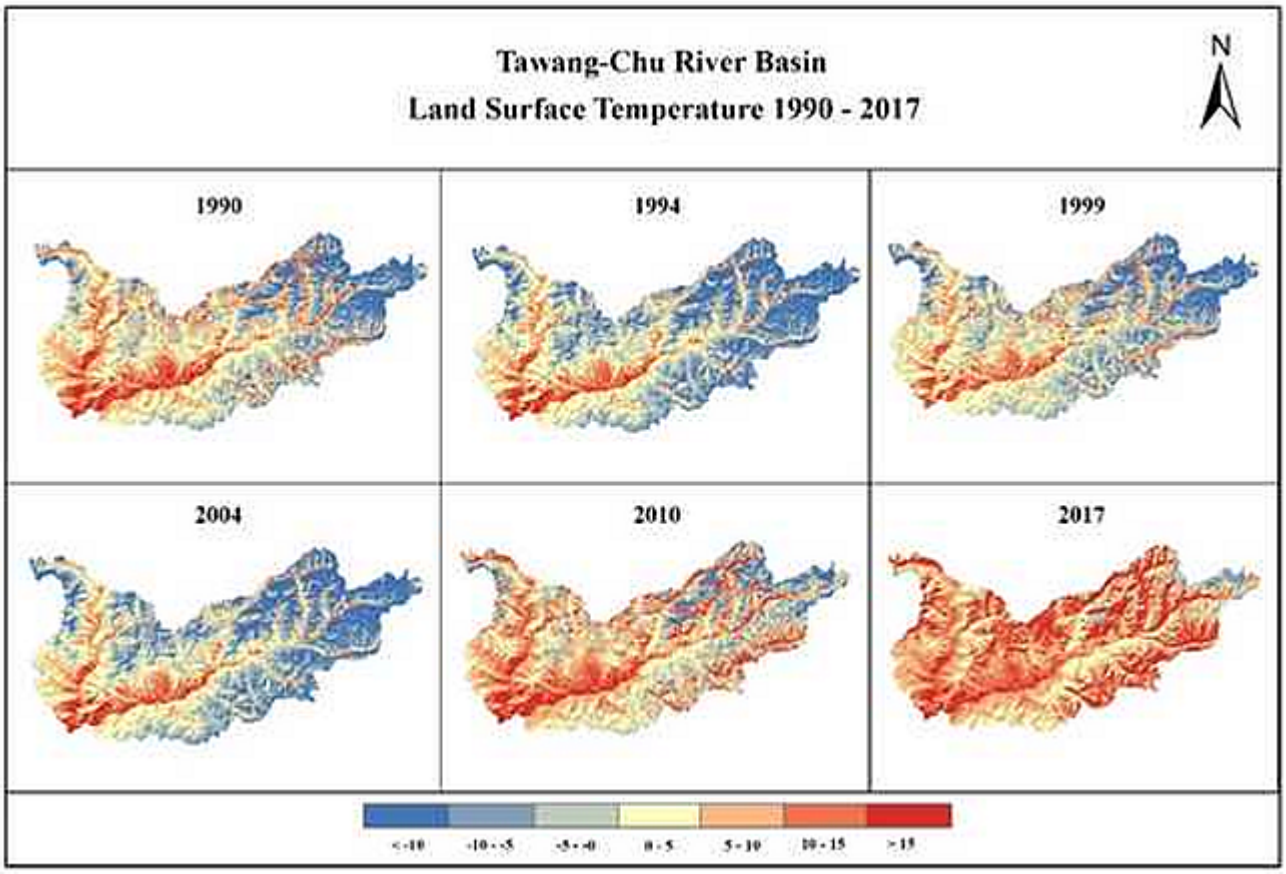


Figure 1. Temporal estimation of LST in year 1990, 1994, 1999, 2004, 2010 and 2017 of Tawang-Chu River basin (°C).

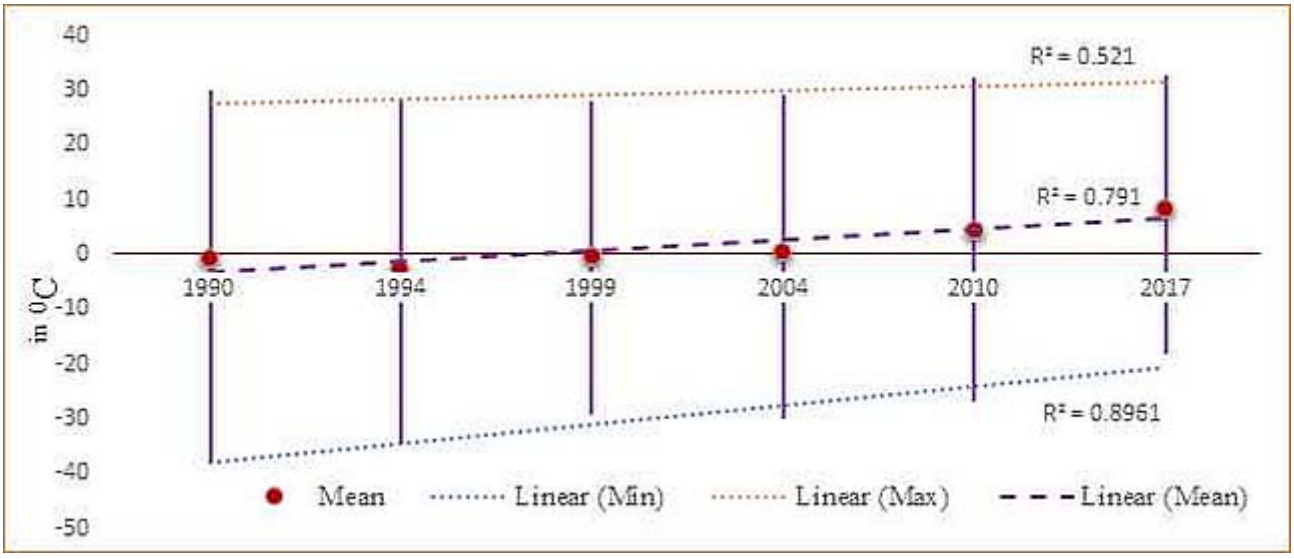


Figure 2. Temporal data extraction of Land surface temperature of Tawang-Chu River basin (1990- 2017 in $^{0}$C).

0.8961 has strong coefficient of determination, which is highly statistically significant. Hence, it can be comparatively significant regarding changing ecological services in the basin because of potentially high-ecological footprint. Enormous changes in the annual mean-value of temperature from a negative (-0.73) to a positive digit (8.54) value reflects a huge temperature change. Besides this, the standard deviation shows how the difference between minimum and maximum temperature is shrinking with an increasing temperature trend in the basin.

**Rainfall trends in the Tawang-Chu River Basin**

Tables 2, 3 and Figure 3 provide a summary of the results from the analysis of rainfall trends in the Tawang-Chu River Basin.

The continuity correction was applied in the analysis of the data. As noted in Table 2, the annual rainfall S value is -219.000, which shows strong decreasing trend in rainfall during 34 years covered by this study, with a p-value of 0.001 < 0.05 (alpha), implying a highly statistically significant trend in annual rainfall received in the Tawang-Chu River Basin. In the summer season, S value is -71.000, which shows a relatively low decreasing trend in rainfall during the same period, with a p-value of 0.299 < 0.05 (alpha), indicating a statistically insignificant trend in summer rainfall within the basin (Table 3).

The results indicate that the rainfall that was received during the Monsoon season had an S value of -309.000, which shows a very strong decreasing trend in the rainfall amounts that were recorded during the 34 years that were covered by this study, with a p-value of 0.0001 < 0.05 (alpha), implying a highly statistically significant trend in Monsoon rainfall within the Tawang-Chu River Basin. The S value for the winter season is 136.000, which shows increasing/ positive trend in rainfall over the 34-year period, with a p-value is 0.045 < 0.05 (alpha), suggesting a statistically significant trend in winter rainfall within the basin.

To estimate the magnitude of trend (slope of trend) of the annual rainfall; daily data of rainfall amount has been used and output values -22.849 shows descending slope of curve and the magnitude of trend (slope of trend) summer rainfall data output values is -3.867 which shows descending but weak slope of curve. The magnitude of trend (slope of trend) of Monsoon monthly rainfall shows a descending slope of -20.386 while estimated the magnitude of trend (slope of trend) of winter monthly rainfall output value is 1.536 shows an ascending trend (Table 4).

The $R^2$ value for annual rainfall trend is **0.379 (**p <0.0001**),** which is statistically lesser significant. It indicates about 37% of variability in the annual rainfall in Tawang-Chu River Basin. In the Summer

Table 2. The rainfall characteristics of the Tawang-Chu River Basin

| Variable | Observations (N) | Minimum (mm) | Maximum (mm) | Mean (mm) | Std. deviation |
|---|---|---|---|---|---|
| Annual Rainfall | 34 | 1236.00 | 2791.40 | 2045.43 | 378.14 |
| Summer Rainfall | 34 | 487.80 | 1216.00 | 839.89 | 165.26 |
| Monsoon Rainfall | 34 | 624.00 | 1835.11 | 1143.30 | 290.27 |
| Winter Rainfall | 34 | 9.831 | 152.000 | 62.243 | 44.026 |

Table 3. Mann-Kendall trend test / Two-tailed test (Annual Rainfall in mm)

| | Annual Rainfall | Summer Rainfall | Monsoon Rainfall | Winter Rainfall |
|---|---|---|---|---|
| Kendall's tau | -0.390 | -0.127 | -0.551 | 0.243 |
| S | **-219.000** | -71.000 | **-309.000** | **136.000** |
| Var(S) | 4550.333 | 4550.333 | 4550.333 | 4549.333 |
| p-value (Two-tailed) | **0.001** | 0.299 | **< 0.0001** | **0.045** |
| alpha | 0.05 | 0.05 | 0.05 | 0.05 |

An approximation has been used to compute the p-value.

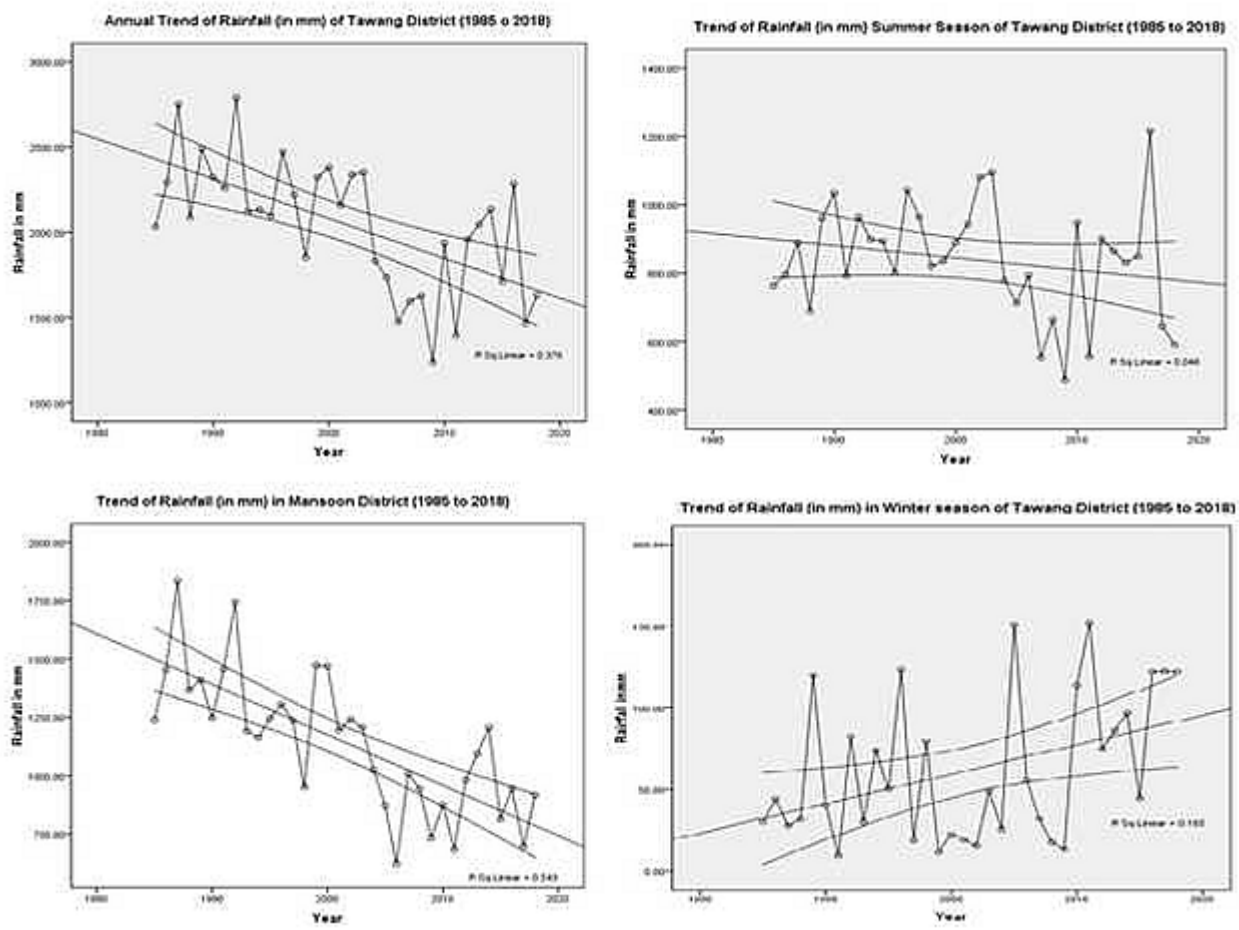


Figure 3. Annual trend of Rainfall in Tawang-Chu River Basin

Table 4. Sen's slope: Annual Rainfall

| Seasons | | Value | Lower bound (95%) | Upper bound (95%) |
|---|---|---|---|---|
| Annual Rainfall | Slope | -22.849 | -36.042 | -10.601 |
| | Intercept | 47752.378 | 35511.230 | 60957.786 |
| Summer Rainfall | Slope | -3.867 | -10.440 | 2.569 |
| | Intercept | 8589.001 | 2149.863 | 15155.718 |
| Monsoon Rainfall | Slope | -20.386 | -28.182 | -14.120 |
| | Intercept | 41931.346 | 35675.507 | 49736.975 |
| Winter Rainfall | Slope | 1.536 | 0.018 | 3.118 |
| | Intercept | -3017.522 | -4599.851 | -1503.301 |

Season, variability of rainfall is unpredictable as $R^2$ value is 0.046 ($p>0.0001$), which suggests that there the variability in rainfall for this season is not statistically significant. The $R^2$ value for the Monsoon Season is 0.55 ($r = 0{,}742$, $df = 33$ $p < 0.0001$), which is highly statistically significant. The $R^2$ value for the Winter Season is 0.165, i.e., $r = r = 0.406$ ($p = 0.0155$), which is statistically significant.

**Physiographical conditions within the Tawang-Chu River Basin**

***Variability of NDVI Values and Land Use Land Cover (LULC) Changes in the Tawang- Chu River Basin***

As shown in the results of this study, NDVIs values show that density of vegetation in the Tawang-Chu

River Basin is gradually decreasing, while the area covered by vegetation is increasing (Fig. 4). In 1990 the "greenness" of dense evergreen forest was much higher than in subsequent years (as indicated by the NDVI value of 0.89), but over the years the coverage of the green less area has been decreasing gradually (Fig. 5). On the one hand, while the continuous declining trend in maximum values of NDVI can be noticeable, the minimum values of NDVI have also been declining rapidly. The area under the vegetation cover is constantly shrinking. Similarly, the area covered by surface water and snow is showing a shrinking trend. The increasing vegetated area and the declining of the area covered by snow and surface water can be interpreted as a significant sign of a rising tree line the river basin. In 2017, the maximum NDVI was 0.51, which signifies presence of shrub or grassland cover, evidence of declining vegetation density (Fig. 5). As discussed below, in the Tawang-Chu River Basin, changes in NDVI values were accompanied by LULC changes.

Landsat (L4, L5, L7 and L8) images for the years included in this study were analysed in order to assess the LULC changes that took place between 1990 and 2017**.** The Landsat satellite images were converted to False Colour Composites (FCCs) and then a geo-referenced to provide geographic projection using ArcGIS software. Thereafter, the maximum likelihood technique was used to define the supervised classification of all zones into three classes - vegetation, uncultivated or wasteland, and snow-cover (Table 8). After that, ground validation and editing of the initial LULC maps was done using ArcGIS software. For assessing Kappa accuracy, the graded points were compared by randomly indicated original images (Table 5). Later, the next step was the calculation of the LULC and the classification of the basin into defined classified divisions or types of land cover.

The final step involved the comparative analysis of changes of LULC areas that were computed (Fig. 6). Based on the results shown in Table 5, it can be concluded that there is an increasing trend in vegetation and fallow / wastelands, while snow and glaciers are steadily declining (Fig. 7). Fallow and barren land contains the whole inhabited area, including all other indicators of land use (Table 5). The increase of fallow land indicates that the land is being abandoned due to loss of productivity, a phenomenon which has the potential to worsen food insecurity in the Tawang-Chu River Basin.

All other indicators of land use like the inhabited area, cultivated land and other land uses were difficult to identify with precision using the methods that were applied in study due to the very rough geographical landscape because when it was being done, it was

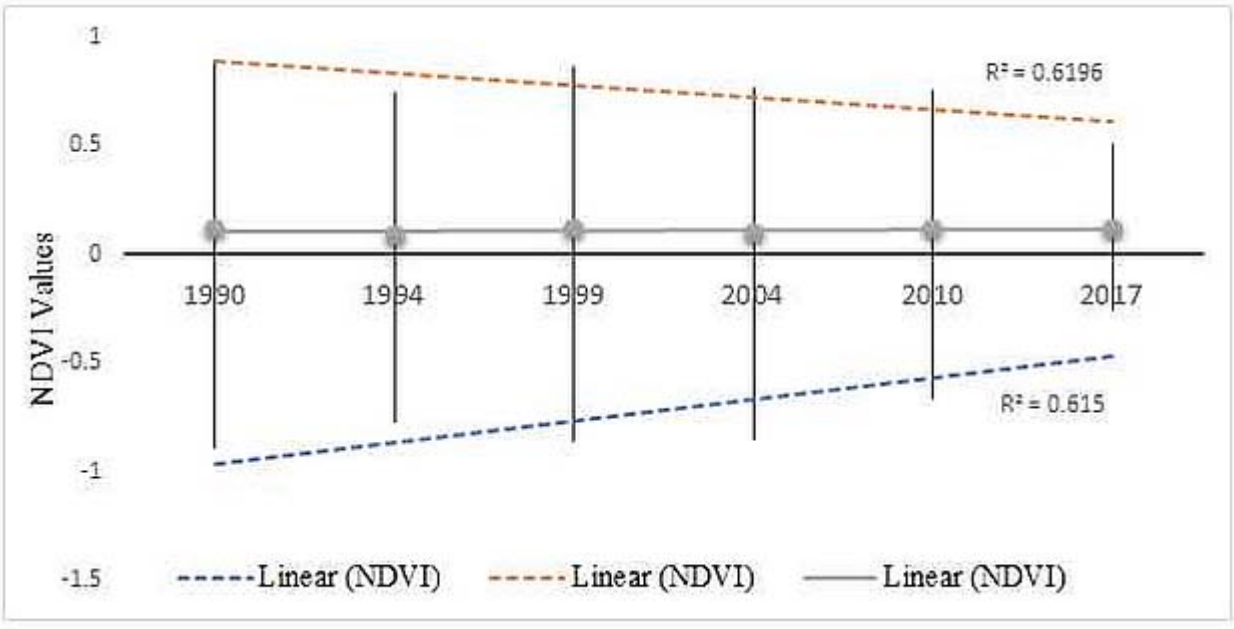


Figure 4. Temporal data extraction Values of NDVI of Tawang-Chu River basin (1990-2017)

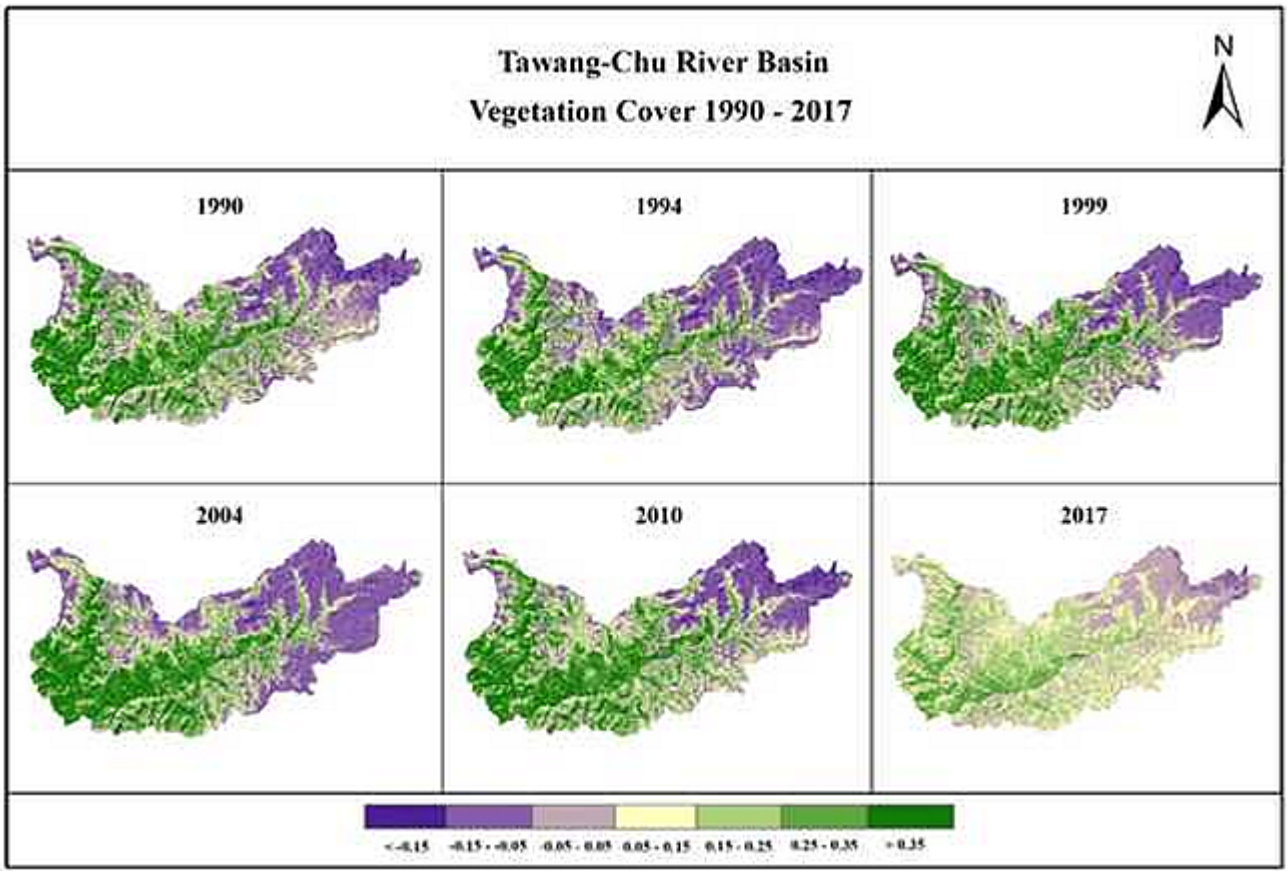


Figure 5. Normalized Difference Vegetation Index (NDVI) of Tawang-Chu River Basin

Table 5. LULC Changes in Tawang District during 1990 to 2017

| Land Classification (in km$^2$) | 1990 | 1994 | 1999 | 2004 | 2010 | 2017 |
|---|---|---|---|---|---|---|
| Vegetation Cover Area | 12045.528 | 10625.094 | 12663.27 | 10417.14 | 12627.36 | 14067.117 |
| Barren/ Fallow/ other land | 9835.799 | 6648.498 | 7910.388 | 9119.619 | 9155.61 | 9868.536 |
| Snow Cover Area | 2962.345 | 7570.08 | 4270.014 | 5306.913 | 3060.702 | 908.019 |
| Total Land | 24843.672 | 24843.672 | 24843.672 | 24843.672 | 24843.672 | 24843.672 |

going to be very messy and the chances of getting inaccuracies were high. Therefore, Settlements area, Agricultural land and other land use types not marked as an indicator. The Tawang-Chu River Basin is a restricted area whose access is controlled by the Indian Army, and identification of inhabited areas was only achieved through satellite for academic research and other purpose is prohibited.

Increase in the area covered by vegetation and fallow land (including other land use) and decreasing trends in snow-covered land are indicative of changing physio-climatic conditions. This has been caused by a rapid rise in minimum temperatures, which has been confirmed by the estimated LSTs. According to the results presented above, it can be argued that during the 27-year study period, tough the average temperature has been rising gradually rising, the minimum temperature has been increasing rapidly. The gradually and rapidly declining trends of LST and NDVI values, respectively, are evidence showing a strong positive relation between LST and NDVI values (Fig. 6). These results mean that changes in NDVI values are a direct response of vegetation to LST values within the Tawang-Chu River Basin. As temperature increases, the area and nature of vegetation also change accordingly (Fig. 6). $R^2$ values ranging between 0.93 to 0.99, mean the coefficient of determination values are a

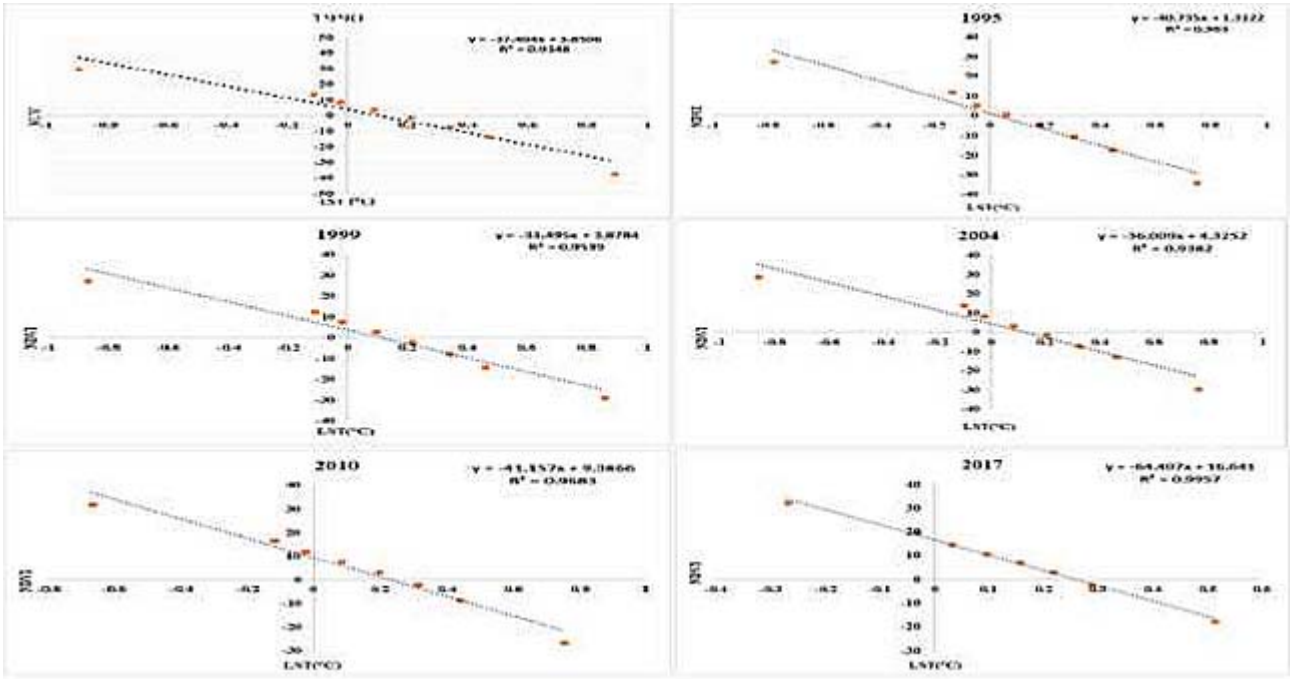


Figure 6. Linear Regression with Scatter Plots of LST and NDVI of Tawang River Basin

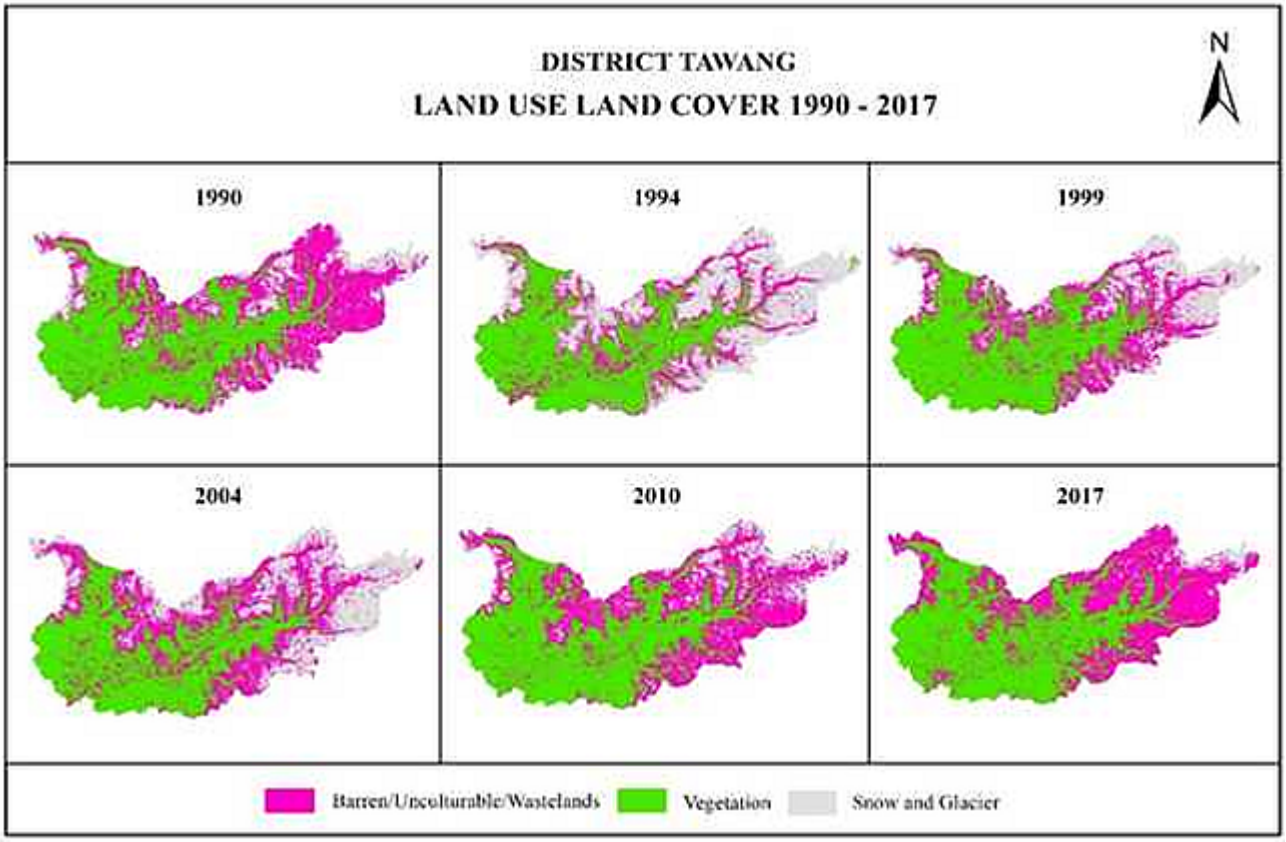


Figure 7. LULC (1990) Map of Tawang District, 2020

reflection of a strong interdependence on each other. The positive changes in temperature have a negative effect on precipitation, as both the amount and duration of snowfall is decreasing, while the amount of rainfall is decreasing. Also, the period over which rainfall is received is generally increasing, while the

period over which snowfall occurs has been partly modified into the rainfall period.

A rapid rise in minimum temperature has been continuously reducing both the duration and quantity of snowfall, causing the shrinking of glacial / snowy area and the increase of the fallow land (Table 5).

Figure 8. Trend of LULC Change (1990 - 2017) of Tawang District, 2020

The continuous increase in daily maximum temperature has also caused a change in the rainfall period, the effect of which can be seen as an increase in the area under vegetation cover, even though there was a declining trend in rainfall (Fig. 8).

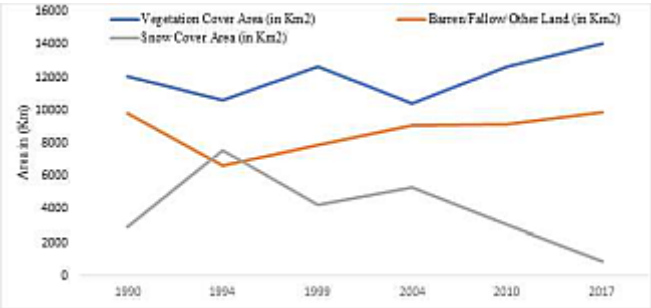


## CONCLUSION

LST data show that minimum temperature is increasing rapidly in the study area although the maximum temperature is rising gradually. The rate of increment for maximum temperature is comparatively lower than that of minimum temperature. The standard deviation for temperature range shows a decreasing trend, which means that the difference between the minimum temperature and maximum temperature is decreasing. Using the Mann-Kendall trend test, it was observed that there is an increasing trend of rainfall in the winter season and no trend was observed in the summer season. Annual and monsoon rainfall data exhibited positive trends. The NDVI values of the study area show that the area covered by dense vegetation is declining gradually, though the total vegetated area is increasing. For example, in 1990 the amount of dense evergreen forest was higher (as NDVI value is 0.89) than in subsequent years, but green less area was decreasing gradually in the subsequent years. These changes have a major impact on LULC patterns in the Twang-Chu River Basin. Comparative analysis of NVDI and LST shows that both indices have a similar pattern of the trend as those of the increasing temperature, while LULC analysis show that, vegetation area is increasing, even though there is no clear trend exhibited. In the Tawang-Chu River Basin, the snow cover area is decreasing while baren land/ fallow land is showing an increasing trend.

In can be concluded that changing pattern of temperature in the mountain ecosystem of the Twang-Chu River Basin has altered the ecological processes and inter-ecological nexus of the basin. It can also therefore be concluded that in the Tawang-Chu River Basin natural resources and related ecosystem services are shaped by climate change. The adverse effect of changing variables in of this mountain region may create a fragile environment in in the future. Consequently, we can be concluded that the mountain ecology of Tawang-Chu River Basin is facing a threat from climate, which is not only creating problems for humans but also for the entire biome in the valley.

## ACKNOWLEDGEMENTS

Corresponding author acknowledges the Funding of University Grant Commission (UGC), Government of India for JRF/SRF fellowships. Authors are thankful to the Department of Geography, Delhi School of Economics, University of Delhi and MECESUP UCT 0804 project for providing institutional resources to complete this paper. We thank to Mr. Ambrish who provide us technical help to collect required data used in this paper.

**Authors' Contributions:** All authors contributed equally

**Conflict of interest:** Authors declare no conflict of interest

## REFERENCES

Becker, F. and Li, Z.-L. 1990. Temperature independent spectral indices in thermal infrared bands. Remote Sensing of Environment, 32, 17 – 33.

Beniston, M., Diaz, H.F. and Bradley, R.S. 1997. Climatic Change at High Elevation Sites; A Review', Climate. Change, 36, 233–251. DOI: 10.1023/A:1005380714349

Berk, A., Bernstein, L.S. and Robertson, D.C. 1989. MODTRAN: A Moderate Resolution Model for LOWTRAN 7, Technical Report GL-TR-89-0122, Geophysics. Lab, Bedford, M A.

Buishand, T.A. 1982. Some Methods for Testing the Homogeneity of Rainfall Records. Journal of Hydrology, 58(1-2), 11-27. DOI: 10.1016/0022-1694(82)90066-X

Carlson, T.N. and Ripley, D.A. 1997. On the relation between NDVI, fractional vegetation cover, and leaf area index. Remote Sensing Environment, 62, 241–252.

Chasie, M., Theophilus, P.K. and Rocky, W.S. 2013. Macro-scale landslide hazard zonation along National Highway corridors between Bomdila and Tawang, West Tawang and Tawang Districts, Arunachal Pradesh. GSI Report for FS 2012-13.

Chavez, P.S. 1996. Image-based atmospheric correction. Photogrammetric Engineering and Remote Sensing, 62(9), 1025 – 1036.

Corbet, G.E. and Hill, J.E. 1992. The Mammals of the Indo-malayan Region: A Systematic Review. Oxford University Press, New York, USA.

Diaz, H.F. and Bradley, R.S. 1997. Temperature variations during the last century at high elevation sites. Climate Change, 36, 253–279 DOI: 10.1023/A:1005335731187

Diaz, H.F., Grosjean, M. and Graumlich, L. 2003. Climate variability and change in high elevation regions: past, present and future. Climate Change, 59, 1–4. DOI: 10.1023/A:1024416227887

District Statistical Handbook. 2015-16. Director Directorate of Economics and Statistics. Government of Arunachal Pradesh, Tawang District. Tawang.

District Statistical Handbook. 2018-19. Director Directorate of Economics and Statistics. Government of Arunachal Pradesh, Tawang District. Tawang.

Dussaillant, I., Berthier, E., Brun, F., Hugonnet, R., Favier, V., Rabatel, A., Pitte, P. and Ruiz, L. 2019. Two decades of glacier mass loss along the Andes. Nature Geosscience, 12, 802-808. DOI: 10.1038/s41561-019-0432-5

Fischlin, A. and Bugmann, H. 1994. Comparing the Behaviour of Mountainous Forest Succession Models in a Changing Climate. Pp. 204–219. In: Beniston, M. (Ed.), Mountain Environments in Changing Climates, Routledge Publishing Company, London and New York.

Fuhrer, J., Beniston, M., Fischlin, A., Frei, C., Goyette, S., Jasper, K. and Pfister, C. 2006. Climate risks and their impact on agriculture and forests in Switzerland. In: Climate Variability, Predictability and Climate Risks. Springer Netherlands, 79(1-2), 79–102.

Gomis-Cebolla, J., Jimenez, J.C. and Sobrino, J.A. 2018. LST retrieval algorithm adapted to the Amazon evergreen forests using MODIS data. Remote Sensing of Environment, 204, 401-411 DOI: 10.1016/j.rse.2017.10.015

Herold, M., Latham, J.S., Di Gregorio, A. and Schmullius, C.C. 2007. Evolving Standards in Land Cover Characterization. Journal of Land Use Science, 1(2-4), 157-168. DOI: 10.1080/17474230601079316

Hollander, M. and Wolfe, D.A. 1973. Nonparametric Statistical Methods. John Wiley & Sons, New York. DOI: 10.1002/bimj.19750170808

ICIMOD. 2008. Recorded proceedings of the two day Climate Change and Vulnerability of Mountain Ecosystems in the Eastern Himalayan Region. North-East India & Bhutan Stakeholders Workshop, 11-12 March, 2008, Shillong. Organised by International Centre for Integrated Mountain Development Kathmandu, Nepal.

IUCN. 2004. IUCN Red List of Threatened Species. IUCN, Gland, Switzerland http://www.redlist.org/info/tables/html [accessed 21 January 2020].

Jones, C. 2019. Recent changes in the South America low-level jet. npj Climate and Atmospheric Sciences, 2, 20. DOI: 10.1029/2003JD003480

Kendall, M.G. 1975. Rank Correlation Methods. Griffin, London, UK.

Kohler, M.A. 1949. On the Use of Double-mass analysis for testing the consistency of records and for making adjustments. Bulletin of the American Meteorological Society (BAMS), 30, 188–19. DOI: 10.1175/1520-0477-30.5.188

Kohler, T., Giger, M., Hurni, H., Ott, C., Wiesmsnn, U., Dach, S.W. and Maselli, D. 2010. Mountains and climate change: a global concern. Mountain Research and Development, 30(1), 53-55. DOI: 10.1659/MRD-JOURNAL-D-09-00086.1

Laraby, K.G. and Schott, J.R. 2018. Uncertainty estimation method and Landsat 7 global validation for the Landsat surface temperature product. Remote Sensing of Environment, 216, 472-481. https://doi.org/10.1016/j.rse.2018.06.026

Lehmann, E.L. 1975. Nonparametrics, Statistical Methods Based on Ranks. Holden-Day, San Francisco, California, USA.

Li, Z.L., Xu, Z.X., Li, J.Y. and Li, Z.J. 2008. Shift trend and step changes for runoff time series in the Shiyang River Basin, Northwest China. Hydrological Processes, 22(23), 4639–4646. DOI: 10.1002/hyp.7127

Liu, C., Shi, J., Wang, T., Ram, K. and Zhao, T. 2019. Mathematical assessment of the effects of substituting the band radiative transfer equation (RTE) for the spectral RTE in the applications of the Earth's surface temperature retrievals from spaceborne infrared imageries. Remote Sensing, 11(3), 226. DOI:10.3390/rs11030226

Longobardi, A. and Villani, P. 2010. Trend analysis of annual and seasonal rainfall time series in the Mediterranean area. International Journal of Climatology, 30(10), 1538–1546. DOI: 10.1002/joc.2001

Mallick, S., Dutta, S. and Min, K-H. 2017. Quality assessment and forecast sensitivity of global remote sensing observations. Advances in Atmospheric Sciences, 34, 371-382. DOI: 10.1007/s00376-016-6109-8

Mann, H.B. 1945. Nonparametric tests against trend. Econometrica, 13(3), 245–259. DOI: 2307/1907187

Marengo, J.A. 2005. Characteristics and spatio-temporal variability of the Amazon River Basin Water Budget. Climate Dynamics, 24, 11-22. DOI: 10.1007/s00382-004-0461-6

Mishra, H. and Pandey, B.W. 2019. Navigating the Impacts of

Social and Environmental Changes to Traditional Lifestyle: A Case Study of Gaddi Transhumance of Chamba District in Himachal Pradesh. The Oriental Anthropologist, 19(2), 326-337.

Modarres, R. and Silva, V.P.R. 2007. Rainfall trends in arid and semi-arid regions of Iran. Journal of Arid Environments, ??, 344–355.

Mohamed, A.A. and Mukwada G. 2020. Temperature Changes in the Maluti-Drakensberg Region: An Analysis of Trends for the 1960-2016 Period. Atmosphere,10(8), 471. DOI: 10.3390/atmos10080471

Nerry, F., Labed, J. and Stoll, M.P. 1998. Emissivity signatures in the thermal IR band for Remote Sensing: calibration procedure and method of measurement. Applied Optics, 27(4), 758 – 764. DOI: 10.1364/AO.27.000758

Nussbaum, E.M. 2015. Categorical and nonparametric data analysis. Routlesge, Taylor & Francis Group, New York and London.

Oguz, H. 2013. LST calculator: A program for retrieving land surface temperature from Landsat TM/ETM+ imagery. Environment Engineering Management Journal, 12, 549–555.

Olivera-Guerra, L., Merlin, O. and Er-Raki, S. 2020. Irrigation retrieval from Landsat optical/thermal data integrated into a crop water balance model: a case study over winter wheat field in a semi-arid region. Remote Sensing of Environment, 239, 111627 DOI: 10.1016/j.rse.2019. 111627

Pandey, B.W. and Prasad, A.S. 2018. Slope vulnerabili-ty, mass wasting and hydrolo-gical hazards in Himalaya: a case study of Alaknanda Basin, Uttarakhand. Terræ Didatica, 14(4), 395-404.

Partal, T. and Kahya, E. 2005. Trend analysis in Turkish precipitation data. Hydrological Processes, 20(9), 2011–2026. DOI: 10.1002/hyp.5993

Prasad, A.S., Pandey, B.W., Leimgruber, W. and Kunwar, R.M. 2016. Mountain hazard susceptibility and livelihood security in the upper catchment area of the river Beas, Kullu Valley, Himachal Pradesh, India. Journal Geoenvironmental Disasters, 3(3), 01-17.

Rahman, D. and Begum, M. 2013. Application of non-parametric test for trend detection of rainfall in the largest Island of Bangladesh. ARPN Journal of Earth Sciences, 2(2), 40–44.

Rahman, H. and Dedieu, G. 1994. SMAC: A simplified method for the atmospheric correction of satellite measurements in the solar spectrum. International Journal of Remote Sensing, 15, 123 – 143. DOI: 10.1080/014311694089 54055

Ranjan, O.J. and Anand, S. 2017. Adaptation and Sustainability in Development: Case Study of Tawang District, Arunachal Pradesh. Pp. 261- 281. In: Pandey, B.W., Negi, V.S. and Kumria, P (Eds.) Environmental Concerns and Sustainable Development in Himalaya. Research India Press, New Delhi.

Ranjan, O.J., Anand, S. and Pandey, B.W. 2016. Understanding cultivation Ecology in Tawang-Chu River Basin Arunachal Pradesh. Pp. 189-203. In: Singh, P. (Ed.) Climate Change and Sustainable Development. Shabdvani Prakashan, New Delhi.

Ranjan, O.J., Anand, S., Pandey, B.W. and Kumria, P. 2020. Spatial analysis of physio-climatic changes and its impact on human adaptation in Tawang Valley: A case study of Monpa Tribe, Eastern Himalaya. The Eastern Anthropologist, 78(1), 125-138.

Romaguera, M., Vaughan, R.G., Izquierdo.Verdiguier, E., Hecker, C.A. and van der Meer, F.D. 2018. Detecting geothermal anomalies and evaluationg LST geothermal component by combining thermal remote sensing time series and land surface model data. Remote Sensing of Environment, 204, 534-552. DOI: 10.1016/ j.rse.2017.10.003

Valor, E. and Caselles, V. 1996. Mapping land surface emissivity from NDVI: application to European, African and South American areas. Remote Sensing of Environment, 57, 167-184. DOI: 10.1016/0034-4257(96) 00039-9

Villaba, R., Lara, A., Boninsegna, J.A., Masiokas, M., Delgado, S., Aravena, J.C., Roig, F.A., Schmelter. A., Wolodarsky, A. and Ripalta, A. 2003. Largescale temporal changes across the southern Andes: 20th century variations in the context of the past 400 years. Climate Change, 59, 177–232 DOI: 10.1023/A:1024452701153

Wald, A. and Wolfowitz, J. 1942. An exact test for randomness in the non-parametric case based on serial correlation. Annual Mathematical Statistics, 14, 378-388.

Wallis, W.A. and Moore, G.H. 1941. A Significance Test for Time Series and Other Ordered Observations. Technical report, National Bureau of Economic Research, New York. 1-67.

Whiteman, C.D. 2000. Mountain Meteorology, Oxford University Press.

Wibig, J. and Glowicki, B. 2002. Trends in minimum and maximum temperature in Poland. Climate Research, 20, 123–133 DOI: 10.3354/cr020123

Yang, X.L., Xu, L.R., Liu, K.K., Li, C.H., Hu, J. and Xia, X.H. 1966. Trend in temperature and precipitation in the Zhangweinan River Basin during the last 53 years. Procedia Environmental Sciences, 13, 1966– 1974. DOI: 10.1016/ j.proenv.2012.01.190

Yaning, C., Changchun, X. and Xingming, H. 2009. Fifty-year climate change and its effect on annual runoff in the Tarim River Basin, China. Quaternary International, 208(1-2), 53–61. DOI: 10.1016/j.quaint.2008.11.011

Zar, J.H. 2010. Biostatistical Analysis. Prentice

*Received:31st July 2022*
*Accepted:30th August 2022*